VARIATION LAW OF WATER LEVEL IN WATER INJECTION DRILL UNDER THE INFLUENCE OF MINING IN DATONG MINING AREA

by

Feng DU, Yang GAO, Zhen-Hua LI*, Wen-Qiang WANG, and Guo-Sheng LI
School of Energy Science and Engineering, Henan Polytechnic University, Jiaozuo, China

Original scientific paper
https://doi.org/10.2298/TSCI2106407D

In view of the variation law of water level in water injection drill between double-system layers of hard rock strata in Datong mining zone, the failure process and mechanism of boreholes during propulsion are analyzed by the numerical simulation and the test measurement in this paper. After the coal seam is fully mined, it can be divided into the advanced deformation zone, the bending deformation zone and the compaction stable zone. Borehole damage intensifies from top to bottom. The junction of siltstone and sandy mudstone is a high-risk position. The results are verified by the water level measurement and the borehole peeping.

Key words: *water injection drill, water level, mining influence, borehole peeping, Datong mining area*

Introduction

With the application and development of shale gas, coal, oil and gas extraction and underground coal gasification technology at home and abroad, the deformation of vertical borehole and the gas leakage have brought great threats to the safety production [1, 2]. According to related statistics, the damage of ground drilling caused by coal mining occurred in China, and the United States, resulting in great economic losses [3, 4]. Because the boreholes are mostly located above the working face, which are prone to various forms of deformation failure such as shear, tilt, stratification and compression under the influence of mining [5, 6]. Therefore, it is of great significance to carry out the in-depth study on deformation process and characteristics of boreholes under the influence of mining [7, 8].

At present, lots of the problems in the vertical drilling failure have been done by scholars at home and abroad [9, 10]. Peng *et al.* [11] studied the high-risk damage section of ground drilling, and studied the damage mechanism through numerical simulation. Whittles *et al.* [12] analyzed the failure form of borehole by studying the failure law of gas extraction borehole during coal seam mining, and proposed the S-shaped model of shear deformation. Sun *et al.* [13] analyzed the law of inter-layer shear slip and squeezing deformation of overlying strata, and put forward the design basis of engineering protection measurement for drilling.

The aforementioned research results reveal the influencing factors and failure modes of borehole, but seldom analyze the failure process, failure modes and the location of vertical drilling in the mining process [14]. Therefore, on the basis of the relevant researches, this paper explores the variation law of water level in water injection drill between double-system layers of hard rock strata in Datong mining zone, and analyzes the damage process, damage form and

* Corresponding author, e-mail: jzlizhenh@163.com

damage location of the borehole during the advancement process, which are verified by test measurement and borehole peeping.

Mining conditions

The Datong mine is located about 20 km southwest of Datong city, northeast of Datong coalfield, 10.36 km wide from north to south of the mine field, 14.29 km from east to west, and covering an area of 85.12 km^2. The Datong coal field is a dual-series coal seam area. There are Jurassic and Carboniferous dual-series coal seams in the mining area. This paper takes 8309 working face as the research background. The drilling histogram of 8309 working face is shown in fig. 1. The coal seam thickness of 8309 working face is 10.8~18.00 m, and the inclined length is 2843 m. Drill hole 1 is arranged in the middle of the mined-out area. Drill hole 2 is located about 27 m southeast of drill hole 1.

Model establishment and numerical simulation

Establishment of numerical model

With the improvement of computational simulation technology, numerical simulation technology has been widely employed in rock mechanics and engineering practice. The FLAC3-D is professional software to simulate different geological materials to reach the strength limit or yield limit [15, 16]. The mechanical behaviour of failure or plastic flow occurs at the time. It is used to analyse the progressive failure and instability, especially the deformation failure. In order to study the drilling failure process in Datong mining area, this paper uses FLAC3-D to carry out the numerical simulation, and the numerical model size is designed as 900 m × 400 m × 330 m, with a total of 124632 units. There are 100 m coal pillars left and right in the direction of the coal seam, and 100 m coal pillars in the front and back, and a hole with a diameter of 0.2 m at 400 m. With reference to the rock strata in fig. 1, the model diagram is shown in fig. 2.

The boundary of the numerical model is horizontally constrained by the front, back, left, and right boundary in the displacement constraint model. The initial horizontal displacement of the boundary is zero, the horizontal and vertical initial displacements of the bottom boundary are zero, and the top boundary is a free boundary, with 8 MPa load applied on the top boundary. The constitutive model of coal seam adopts elastic-plastic mechanical model, and its failure criterion adopts the Mohr-Coulomb criterion and the tensile stress criterion. With reference to the rock mechanics test, the mechanical parameters of coal and rock mass in the 8309 working face is obtained in tab. 1.

Table 1. Mechanical parameters of coal and rock mass

Lithology	Density, ρ	Bulk modulus, K	Shear modulus, G	Cohesion, c	Tensile strength, σ_b	Internal friction angle, φ
Unit	[kgm^{-3}]	[GPa]	[GPa]	[MPa]	[MPa]	[°]
Medium grain sandstone	2534	11.5	9.2	9.8	4.9	35
Fine sandstone	2595	14.3	12	12.8	5.2	28
Siltstone	2604	19.4	15.3	15.32	4.3	34
Gravel coarse sandstone	2527	14.6	10.07	8.88	5.73	44
Mudstone	2547	10.92	8.5	4.3	3.3	31
Coarse-grained sandstone	2540	7.68	6.23	13.091	4.053	38
Sandy Mudstone	2470	11.41	8.39	8.3	4.7	33
Coal	1426	5.4	4.0	0.89	0.46	26

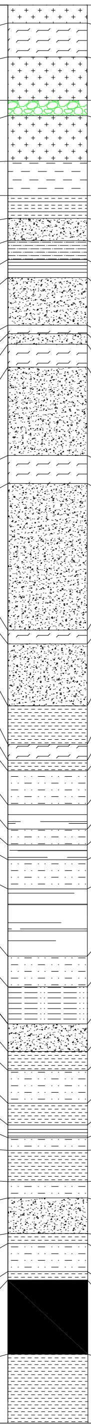

Stratum	Lithology	Columnar	No.	Thickness [m]	Burial depth [m]	Key strata location
Jurassic	Siltstone		1	3.4	342.7	
	Fine-grained		2	6.4	346.1	
	Siltstone		3	8.2	354.3	
	Coals 14		**4**	**2.9**	**357.2**	
	Siltstone		5	8.6	365.8	
	Sandy mudstone		6	6.5	372.3	
	Medium-graine		7	4.3	376.6	
	Mudstone		8	4.2	380.8	
	Coarse-grained		9	3.6	384.4	
	Medium-graine		10	3.4	387.8	
	Mudstone		11	9.1	396.9	
	Fine-grained		12	1.6	398.5	
	Mudstone		13	2.0	400.5	
	Fine-grained		14	4.3	404.8	
	Mudstone		15	17.3	422.1	
	Fine-grained		16	5.3	427.4	
	Siltstone		17	27.7	455.1	
	Fine-grained		18	2.6	457.7	**Far-field key strata**
	Siltstone		19	11.7	469.4	
	Sandy mudstone		20	7.3	476.7	
	Fine-grained		21	3.0	479.7	
	Sandy mudstone		22	2.0	481.7	
	Coarse-grained		23	6.4	488.1	
	Coarse sandstone		24	4.6	492.7	
	Coarse-grained		25	3.2	495.9	
	Coarse sandstone		26	2.8	498.7	
	Coarse-grained		27	5.5	504.2	
	Coarse sandstone		28	12.7	516.9	**Near-field key strata**
	Coarse-grained		29	5.8	522.7	
	Coarse sandstone		30	7.0	529.7	
	Mudstone		31	5.2	534.9	
Permian	Sandy mudstone		32	3.6	538.5	
	Coarse-grained		33	6.2	544.7	
	Sandy mudstone		34	4.1	548.8	
	Medium-graine		35	2.4	551.2	
	Coarse-grained		36	2.4	553.6	
	Sandy mudstone		37	5.9	559.5	
	Coarse-grained		38	3.1	562.6	
	Mudstone		39	6.7	569.3	
	Sandy mudstone		40	1.9	571.2	
	Coarse-grained		41	5.3	576.5	
	Sandy mudstone		42	1.6	578.1	
Carboniferous	**Coals 3-5**		**43**	**14**	**592.1**	
	Sandy mudstone		44	8.8	600.9	

Figure 1. The drilling histogram of 8309 working face

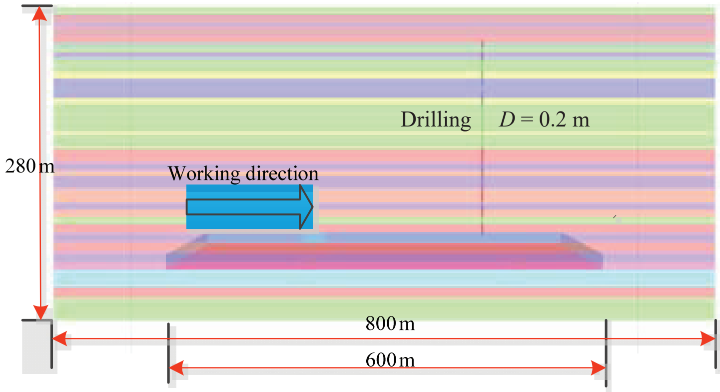

Figure 2. Numerical simulation model diagram

Analysis of drilling failure process

In order to determine the destruction process of the borehole accurately, the changes of the horizontal and vertical displacements of the borehole in different periods are analyzed by the numerical simulation. The size and distribution of horizontal displacement of the borehole is studied, and the size and distribution characteristics of the horizontal displacement of the borehole are obtained. With the advancement of the 8309 working face, the upper part of the drilling hole is slightly inclined, when the drilling hole is pushed through the working face. The inclination is about 0~0.063 m. When the working face advances through the borehole, the borehole begins to move violently and shift horizontally. The shifted surface is between the coarse-grained sandstone and the sandy mudstone, just at the junction of the soft and hard rock layers, besides, the displacement increases with the advancement of 8309 working face, the displacement range is 0.27~0.56 m, and the displacement decreases as the height increases.

The vertical displacement of the borehole during the advancement process are also obtained. When the working face has not advanced through the borehole, the vertical displacement of the borehole is zero. The lateral displacement gradually increases. When the working face advances 40~100 m through the borehole, the borehole has obvious vertical displacement fluctuations. The gravel coarse sandstone (13 m thickness) at 74.7 m and the siltstone (11 m thickness) at 123 m are separated, and the separation is about 3.2~7 m. There is obvious separation and displacement at the junction of hard and soft rock layers, and obvious separation layers appear below thick hard rock layers.

Analysis of the characteristics of borehole failure zone

As the working face advances, the drilling failure pattern changes with the drilling position, and the drilling position during the advancement of the working face is shown in fig. 3. According to the change of the failure mode, the area that affects the borehole is divided into the advanced deformation area, the bending deformation area, and the compaction deformation area. The horizontal displacement of the borehole occurs in the advanced deformation zone. At this time, it is mainly affected by mining stress. The displacement increases with the advancement distance, as shown in fig. 4(a). When the borehole is advanced to the bending-deformation zone, the vertical distance starts to increase, but the vertical displacement between the layers is different, and the lower displacement is much larger than the upper displacement. The delamination displacement inclines to the mined-out area, and the rock layer in the same layer is broken; besides, the borehole is compressed between the layers, as shown in fig. 4(b). When the

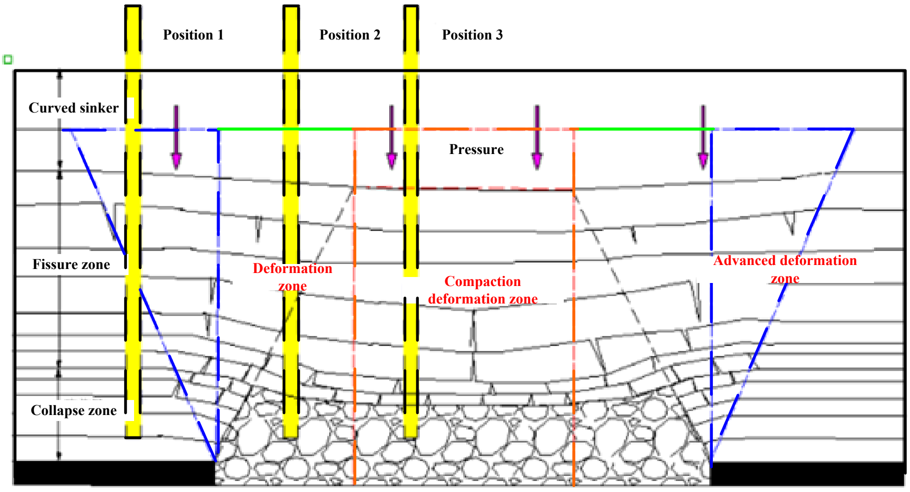

Figure 3. Schematic diagram of the drilling position during the advancement of the working face

horizontal displacement continues to increase, the layer-to-layer separation occurs, as shown in fig. 4(c). When the borehole enters the compaction deformation zone, the borehole failure tends to be stable, and the horizontal and vertical deformations are basically stable.

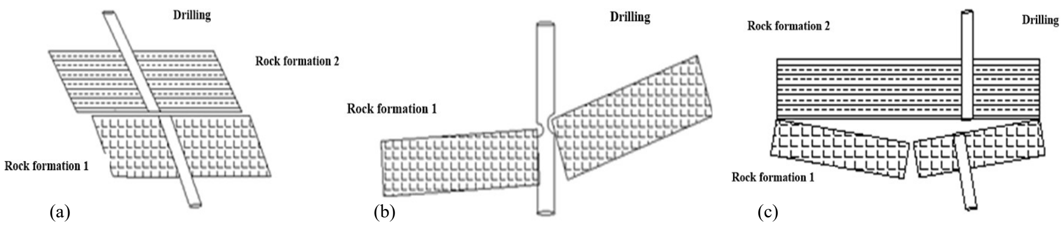

Figure 4. Schematic diagram of drilling failure types; (a) borehole deformation, (b) drilling necking deformation, and (c) borehole destabilization

The borehole is dominated by the inter-layer compression deformation and the inter-layer compression deformation. When the borehole enters the bending deformation zone and the compaction deformation zone, the lower collapse zone begins to collapse, and the borehole breaks into a sinking disordered extrusion. The vertical and horizontal displacements fluctuate violently. The horizontal displacement is the dominant factor, and the vertical displacement decreases with the increasing height. The bending deformation zone is dominated by the small horizontal displacement deformation. As the drilling process progresses, the collapse zone fills completely and tends to be stable. The borehole deforms sharply in the bending deformation zone, and the degree of deformation reaches the maximum value in the compaction deformation zone. The variation characteristics of the three belts are obviously different.

Test verification

Water level changes in the drill hole of water injection

The water level monitoring device is installed on the 1# drill hole. As shown in fig. 5, the 1# drill hole is located in the middle position, which is in the front of the 8309 working surface,

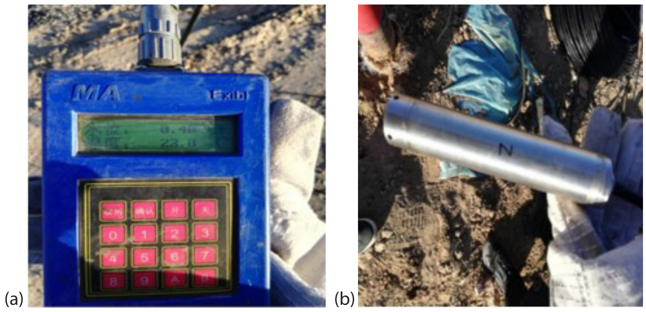

Figure 5. The monitoring device for water level; (a) handhold water level monitor and (b) pressure sensor

and the initial water level monitoring probe is located 57.62 m below the water level in the drill hole of water injection.

At first, the water level is at the slow descending stage. When the 8309 working face is between 232.6~136.6 m away from the 1# water level monitoring hole, the water level in the drilling hole descends at a rate of 0.1~0.2 m per day. At this time, the borehole passes through the upper part of the advanced deformation area, and receives less stress in the direction of the mined-out area, causing the drop of the water level.

Next, the water level enters the slow ascent stage. Within the range of 132.1 m from the drilling face of the 8309 working face to 5.5 m, the drilling water level increases at a rate of 0.02~0.93 m per day. The borehole continues to be close to the mined-out area. As the distance decreases, the borehole enters the advanced deformation zone. Near the bending-off deformation zone, the borehole is subjected to the increased squeezing force between the rock layers.

At last, the water level reaches the sudden drop stage. In the range of 5.5 m to 85.9 m over the borehole of the 8309 working face, the water level of the borehole drops rapidly. Within the range of 5.5~62.5 m, the borehole water level drops at a rate of 1.5~4.2 m per day, and within the range of 62.5~72.5 m, the borehole water level drops to 18.48~25.7 m per day. At this time, the borehole enters the bending and deformation zone, and the direction and size of the horizontal and vertical deformation changes drastically, resulting in the delamination. A large number of crisscross pore wall cracks appear in the borehole, and the displacement exceeds the borehole diameter.

Borehole view

Drilling and peeping into the No. 2 borehole, as shown in fig. 6, the borehole has been tilted and necked at the boundary between the sandy mudstone and siltstone at a distance of 40 m from the working face, and 123 m from the coal seam. The hole is in the advanced deformation zone, and is caused by mining stress in the direction of the gob. As the working face advances, the mutual shearing action of sandy mudstone and siltstone leads to increased borehole misalignment under the influence of mining stress.

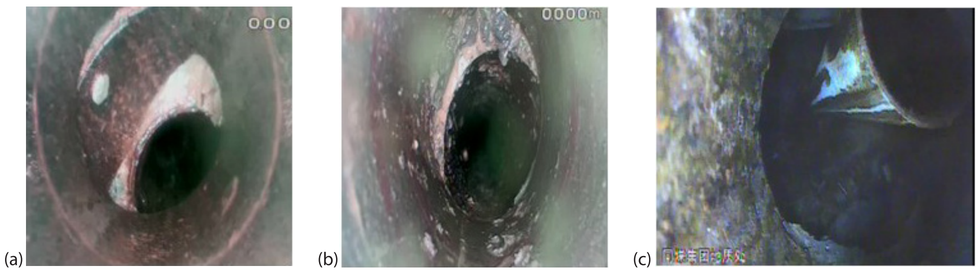

Figure 6. Peep view of drilling damage; (a) borehole deformation, (b) drilling necking deformation, and (c) borehole destabilization

At this time, the horizontal borehole misalignment is obvious. When the working face is advanced to 100 m through the borehole, the shearing effect between the rock layers is intensified. Because the lower rock layer enters the collapse zone, the thick hard siltstone is hinged to the top, resulting in severe horizontal shear and delamination at the junction of the two rock layers above the coal layer. The location of ground drilling damage is prone to appear at the junction of soft and hard rock formations and special locations should be protected for this special period.

Conclusions

In the present work, the analysis results of drilling failure process by numerical simulation show that the area affecting the borehole is divided into the advanced deformation area, the bending deformation area, and the compaction deformation area. Besides, the horizontal displacement of the borehole occurs in the advanced deformation zone, the borehole deforms sharply in the bending deformation zone, and the degree of deformation reaches the maximum value in the compaction deformation zone. Due to the changes of the water level and peep view in the drill hole of water injection in site test, the mutual shearing action of sandy mudstone and siltstone leads to increased borehole misalignment under the influence of mining stress, the internal-hole dislocation and separation failure are the key factors in the fracture zone, and the location of ground drilling damage is prone to appear at the junction of the soft and hard rock formations.

Acknowledgment

This study is sponsored by the National Natural Science Foundation of China (51774110, U1904128, 51704095), the Program for Science & Technology Innovation Talents in Universities of Henan Province (19HASTIT047), the Science and Technology Project of Henan Province (182102310012), the Fundamental Research Funds for the Universities of Henan Province (NSFRF200302), the Foundation for Higher Education Key Research Project by Henan Province (19A130001).

References

[1] Liu, S. Q., *et al.*, Technology Process and Application Prospect of Underground Coal Gasification, *Earth Science Frontiers*, *23* (2006), pp. 97-102
[2] Dong, M., *et al.*, Research on Coordinated Exploitation for Resources Overlap Area of Oil-Gas and Coal in Ordos Basin, *China Energy and Environmental Protection*, *2* (2017), 19, pp. 101-104
[3] Cao, Z. Z., *et al.*, Joint Bearing Mechanism of Coal Pillar and Backfilling Body in Roadway Backfilling Mining Technology, *Computers, Materials & Continua*, *54* (2018), 2, pp. 137-159
[4] Xue, Y., *et al.*, Analysis of Deformation, Permeability and Energy Evolution Characteristics of Coal Mass around Borehole after Excavation, *Natural Resources Research*, *29* (2020), 5, pp. 3159-3177
[5] Xue, Y., *et al.*, Investigation of the Influence of Gas Fracturing on Fracturing Characteristics of Coal Mass and Gass Exctraction Efficiency Based on a Multi-Physical Field Model, *Journal of Petroleum Science and Engineering*, *206* (2021), Nov., pp. 109018
[6] Jiang, S. Y., *et al.*, Analysis on Comprehensive Protection and Utilization of Resources in Large Onshore Sedimentary Basin, *Natural Resource Economics of China*, *32* (2019), 2, pp. 59-62
[7] Xue, Y., *et al.*, Productivity Analysis of Fractured Wells in Reservoir of Hydrogen and Carbon Based on Dual-Porosity Medium Model, *International Journal of Hydrogen Energy*, *45* (2020), 39, pp. 20240-20249
[8] Ren, B., *et al.*, Deformation and Prevention of Ground Drilling Deformation in Deep Wells with Thick Surface Layer and Pressure Relief Mining – A Case Study of Guqiao Mine in Huainan, *Coal Geology & Exploration*, *46* (2018), 5, pp. 159-166
[9] Liu, J., *et al.*, Numerical Evaluation on Multiphase Flow and Heat Transfer during Thermal Stimulation Enhanced Shale Gas Recovery, *Applied Thermal Engineering*, *178* (2020), Sept., pp. 115554

[10] Shen, J., *et al.*, Study of Methane Drainage Borehole Destruction Induced by Rock Strata Movement, *Safety in Coal Mines*, *41* (2010), 3, pp. 1-4
[11] Peng, S., *et al.*, Borehole Casing Failure Analysis in Unconsolidated Formations: A Case Study, *Journal of Petroleum Science and Engineering*, *59* (2007), 3, pp. 226-238
[12] Whittles, D. N., *et al.*, Influence of Geotechnical Factors on Gas Flow Experienced in A UK Longwall Coal Mine Panel, *International Journal of Rock Mechanics & Mining Sciences*, *43* (2006), 3, pp. 369-387
[13] Sun, H. T., *et al.*, A Model of Shear Slipping of Overlying Strata Under Mining Disturbance, *Rock and Soil Mechanics*, *31* (2010), 2, pp. 609-614
[14] Shen, W. L., *et al.*, Prediction of Relative Displacement for Entry Roof with Weak Plane Under the Effect of Mining Abutment Stress, *Tunnelling and Underground Space Technology*, *71* (2018), Jan., pp. 309-317
[15] Xue, Y., *et al.*, Influence of CH_4 Adsorption Diffusion and CH_4-Water Two-Phase Flow on Sealing Efficiency of Caprock in Underground Energy Storage, *Sustainable Energy Technologies and Assesments*, *42* (2020), 100874
[16] Su, H., *et al.*, Stability Characteristics Analysis of Large Diameter Surface Drilling Wellbore and Engineering Control, *Safety in Coal Mines*, *46* (2015), 11, pp. 189-192

Paper submitted: April 23, 2020
Paper revised: June 29, 2020
Paper accepted: August 9, 2020